mathematics

MDPI

Article

A Mathematical Study of a Semiconducting Thermoelastic Rotating Solid Cylinder with Modified Moore–Gibson–Thompson Heat Transfer under the Hall Effect

Iqbal Kaur [1], Kulvinder Singh [2] and Eduard-Marius Craciun [3,*]

[1] Department of Mathematics, Government College for Girls Palwal, Kurukshetra 136131, India; bawahanda@gmail.com
[2] Computer Science & Engineering Department, University Institute of Engineering & Technology, Kurukshetra University, Kurukshetra 136118, India; ksingh2015@kuk.ac.in
[3] Faculty of Mechanical, Industrial and Maritime Engineering, "Ovidius" University of Constanta, 900527 Constanta, Romania
* Correspondence: mcraciun@univ-ovidius.ro

Abstract: This research aims to investigate photo-thermoelastic interactions in a rotating infinite semiconducting solid cylinder under a high magnetic field acting along its axis with the Hall current effect. The boundary surface is subjected to a variable heat flux generated by an exponential laser pulse. The governing equations are expressed using a new photo-thermoelastic model generalized in the Moore–Gibson–Thompson photo-thermal (MGTPT) heat transfer model for a semiconducting medium. The Moore–Gibson–Thompson (MGT) equation is obtained by introducing a thermal relaxation parameter into the Green–Naghdi (GN III) model. The Laplace transform is utilized to determine the mathematical expressions for the components of displacement, carrier density, temperature field, and thermal stresses in the transformed domain. The numerical inversion technique is used to obtain the expressions in the physical domain. The impacts of thermal relaxations, different theories of thermoelasticity, the Hall current, and rotation on the displacement, temperature, thermal stresses, and carrier density are represented graphically using MATLAB software.

Keywords: semiconducting media; Hall current; modified Moore–Gibson–Thompson heat transfer

MSC: 74F15; 74K10; 44A10

check for updates

Citation: Kaur, I.; Singh, K.; Craciun, E.-M. A Mathematical Study of a Semiconducting Thermoelastic Rotating Solid Cylinder with Modified Moore–Gibson–Thompson Heat Transfer under the Hall Effect. *Mathematics* **2022**, *10*, 2386. https://doi.org/10.3390/math10142386

Academic Editor: Andrey Jivkov

Received: 18 June 2022
Accepted: 5 July 2022
Published: 7 July 2022

1. Introduction

Photo-thermoelastic interactions in semiconducting materials due to laser applications are a wide field of investigation. Normally, semiconductors are neither good conductors nor good insulators. Semiconducting materials behave as conductors when exposed to high-temperature fields. When a high-intensity laser interacts with a semiconductor, the substrate material absorbs internal energy and the irradiated zone releases heat, thus producing a thermoelastic deformation as well as an electronic deformation. Semiconductor materials have been used as nanomaterials in various fields of electronics and electrical engineering. They have an assortment of purposes in current industry, such as VLSI, solar cells, and so forth. Numerous mathematical models have been developed to describe the similarity between thermoelasticity and photo-thermal equations. Modern engineers tend to be more interested in semiconductor materials because of technological advancements.

Duhamel [1] presented the theory of classical uncoupled thermoelasticity. This theory has two limitations. To begin with, the elastic material's state has no connection with the temperature. Moreover, due to the parabolic heat equation, this theory predicts that the temperature travels with an infinite speed, which is again contradictory to physical experiments. Biot [2] proposed the hypothesis of coupled thermoelasticity to conquer these impediments. According to this theory, the heat conduction equations and the equations of elasticity are coupled. However, this theory has shortcomings in that it only predicts heat waves with an unlimited speed of propagation. Cattaneo [3] and Vernotte [4,5] suggested a wider form of the Fourier law for the homogeneous and isotropic medium by introducing relaxation time τ_0 to the heat flux vector to establish a steady state at a point when a temperature gradient is abruptly imposed on it, as follows:

$$\left(1+\tau_0\frac{\partial}{\partial t}\right)\boldsymbol{q}=-K_{ij}\nabla T, \tag{1}$$

Later, the generalized theory of thermoelasticity with one relaxation time was proposed by Lord and Shulman [6] for the particular case of an isotropic body. In this theory, the heat equation is hyperbolic, which gives a finite speed of propagation for temperature.

A more precise version of thermoelasticity theory was then presented by Green and Lindsay [7], who illustrated that the linear heat conduction tensor is symmetric. Dhaliwal and Sherief [8] provided the equations of generalized thermoelasticity for an anisotropic medium. However, Green and Naghdi [9–11] proposed the linear and the nonlinear thermoelastic theories with and without energy dissipation, and further developed the Fourier law as follows:

$$\boldsymbol{q}=-K_{ij}\nabla T-K^{*}_{ij}\nabla\vartheta,\, \dot{\vartheta}=T. \tag{2}$$

"*Based on entropy equality, they proposed three new thermoelastic theories. Their theories are known as the thermoelasticity theory of type I, the thermoelasticity theory of type II (i.e., thermoelasticity without energy dissipation), and the thermoelasticity theory of type III (i.e., thermoelasticity with energy dissipation). On linearization, type I becomes the classical heat equation whereas on linearization type-II, as well as type-III theories, give the finite speed of thermal wave propagation*".

There have been a myriad of academic articles that study and interpret the Moore–Gibson–Thompson (MGT) equation in recent years. Lasiecka and Wang [12] founded their theory on a third-order differential equation, which is important for various fluid dynamics. Using the MGT equation with 2T, Quintanilla [13,14] devised a novel heat conduction model. With the MGT equation, the modified Fourier law is:

$$\left(1+\tau_0\frac{\partial}{\partial t}\right)\boldsymbol{q}=-K_{ij}\nabla T-K^{*}_{ij}\nabla\vartheta, \tag{3}$$

where $\dot{\vartheta}=T$.

Fernandez and Quintanilla [15] discussed the linear thermoelastic deformations of dielectrics. Bazarra et al. [16] studied a thermoelastic problem using the MGT thermoelastic equation.

Suppose that the semiconductor elastic media are exposed to external laser beams, which create carrier-free charge density due to excited free electrons with semiconductor gap energy, for example. In response to the absorbed optical energy, there is a change in electronic deformation and elastic vibration. Heat conductivity equations, in this case, will be affected by thermal-elastic-plasma waves. The revised Fourier law for semiconductor materials with plasma impact in a generalized form can be written as:

$$\left(1+\tau_0\frac{\partial}{\partial t}\right)\boldsymbol{q}=-K_{ij}\nabla T-K^{*}_{ij}\nabla\boldsymbol{\vartheta}-\int\frac{E_g\boldsymbol{N}}{\tau}d\boldsymbol{x}, \tag{4}$$

where $\dot{\vartheta}=T$.

The photo-excitation effect is represented by the final term in Equation (9). When the above equation is differentiated with respect to $\vec{x}$, the result is:

$$\left(1+\tau_0\frac{\partial}{\partial t}\right)\nabla.\boldsymbol{q}=-\nabla.\left(K_{ij}\nabla T+K^{*}_{ij}\nabla\boldsymbol{\vartheta}\right)-\frac{E_g\boldsymbol{N}}{\tau}, \tag{5}$$

where $\dot{\vartheta} = T$.

Some other researchers also conducted similar research on the Hall current effect and the semiconductor medium, such as Marin [17], Lata and Kaur [18], Lotfy [19], Mahdy et al. [20], Kaur and Singh [21,22], Marin et al. [23,24], Kaur et al. [25], Bhatti et al. [26,27], Othman and Marin [28], Marin et al. [29], Craciun et al. [30], Lotfy et al. [31], and Abouelregal et al. [32]. However, from the literature review, it was observed that no work has been carried out in the transient study of semiconductor cylinders exposed to ultrashort pulsed laser heating along with the Hall effect and rotation. The importance of this issue is the main motivation for its in-depth review in the present study.

This research aims to study the photo-thermoelastic interactions in a rotating infinite semiconducting solid cylinder under a high magnetic field acting along its axis with the Hall current effect. Variable heat flux in the form of an exponential laser pulse is applied to the boundary surface. The governing equations are expressed using a new photo-thermoelastic model generalized in the MGTPT heat transfer model for a semiconducting medium. The MGT equation is obtained by introducing a thermal relaxation parameter into the Green–Naghdi (GN III) model. The impacts of thermal relaxations, different theories of thermoelasticity, the Hall current, and rotation on the displacement, temperature, thermal stresses, and carrier density are represented graphically using MATLAB software.

2. Basic Equations

Following Mahdy et al. [20], Abouelregal and Atta [33] provided the constitutive relations, the equation of motion, the plasma diffusion equation governing the plasma transportation process in the semiconductor nanostructure medium, the MGTPT heat conduction equation with thermal-plasma-elastic interaction, and the generalized Ohm's law for finite conductivity with the Hall current effect. The modified Ohm's law with the Hall effect for a high strength magnetic field in tensor notation is given by:

1. *Constitutive relations*

$$\begin{aligned} \sigma_{ij} &= (\lambda u_{k,k} - \beta T - \delta_n N)\delta_{ij} + \mu\left(u_{i,j} + u_{j,i}\right), \\ \beta &= (3\lambda + 2\mu)\alpha_t,\ \delta_n = (3\lambda + 2\mu)d_n. \end{aligned} \tag{6}$$

2. *Equation of motion*

$$\sigma_{ij,j} + F_i = \rho\left\{\ddot{u}_i + (\Omega \times (\Omega \times u))_i + 2\left(\Omega \times \dot{u}\right)_i\right\}. \tag{7}$$

3. *Plasma diffusion equation*

$$\frac{\partial N}{\partial t} = D_E \nabla^2 N - \frac{N}{\tau} + \kappa T, \tag{8}$$

where $\kappa = \frac{T}{\tau}\frac{\partial N_0}{\partial T}$.

4. *Modified Moore–Gibson–Thompson heat conduction equation*

$$\left(K_{ij}\dot{T}_{,j}\right)_{,i} + \left(K^*_{ij}T_{,j}\right)_{,i} + \frac{E_g\dot{N}}{\tau} = \left(1 + \tau_0\frac{\partial}{\partial t}\right)\left[\rho C_E\ddot{T} + \beta_{ij}T_0\dot{e}_{ij} - \rho\dot{Q}\right]. \tag{9}$$

where $K_{ij} = K_i\delta_{ij},\ K^*_{ij} = K^*_i\delta_{ij},\ i$ is not summed.

5. *Modified Ohm's law with the Hall effect*

$$J_i = \sigma_0\left(E_i + \mu_0\epsilon_{ijr}\left(u_{j,t} - \frac{\mu_0}{en_e}J_j\right)H_r\right), \tag{10}$$

where $\sigma_0 = \frac{n_e e^2 t_e}{m_e}, m = \omega_e t_e = \frac{\sigma_0\mu_0 H_0}{en_e}, \omega_e = \frac{e\mu_0 H_0}{m_e}$.

Equation (10) can also be written as:

$$J = \sigma_0 \left\{ E + \mu_0 (\dot{u} \times H) - \frac{\mu_0}{e n_e} (J \times H) \right\}.$$

6. *Lorentz force*

$$F_i = \mu_0 \varepsilon_{ijk} J_j H_k, \tag{11}$$

Additionally, the subscript followed by a comma, represents the partial derivative with respect to space coordinates and a superposed dot represents differentiation with respect to the time variable t.

3. Formulation and Solution of the Problem

Consider a one-dimensional (1D), symmetrical, thermally homogenous semiconductor solid cylinder of radius r_0 (Figure 1). An external laser pulse heating system was used to illuminate the external surface of the solid cylinder. A cylindrical coordinate system (r, θ, z) was considered and the z-axis was taken along the cylinder axis. Initially, the cylinder was kept at a constant and uniform (T_0) temperature.

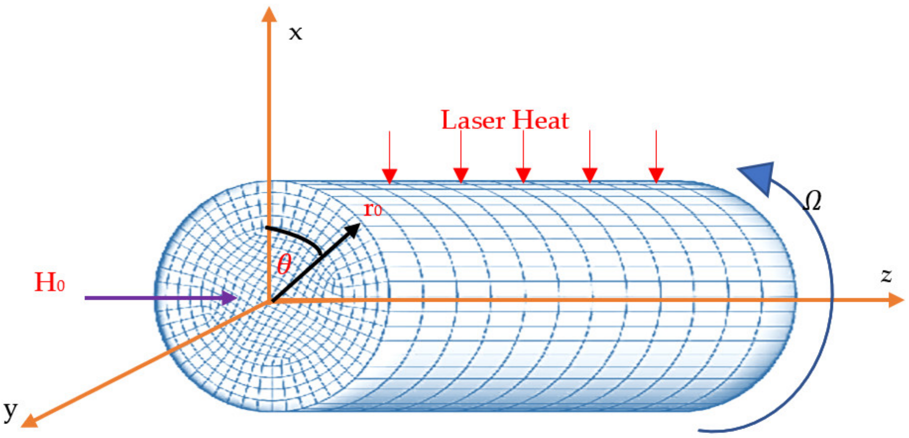

Figure 1. Structure of the problem.

Due to symmetry, for a one-dimensional problem, all the functions considered depend on the radial distance r and time t. For the 1D problem, displacement components and the displacement–strain relations are given by:

$$\boldsymbol{u} = (u, 0, 0)(r, t), \tag{12}$$

$$e_{rr} = \frac{u}{r}, e_{\theta\theta} = \frac{\partial u}{\partial r}, e_{r\theta} = e_{rz} = e_{\theta z} = e_{zz} = 0. \tag{13}$$

The stress–strain–temperature–carrier relations (6) using (12) and (13) will take the form:

$$\sigma_{rr} = 2\mu \frac{\partial u}{\partial r} + \lambda e - (\beta T + \delta_n N), \tag{14}$$

$$\sigma_{\theta\theta} = 2\mu \frac{u}{r} + \lambda e - (\beta T + \delta_n N), \tag{15}$$

$$\sigma_{zz} = \lambda e - (\beta T + \delta_n N), \tag{16}$$

where $e_{kk} = e = \frac{1}{r}\frac{\partial (ru)}{\partial r}$. While using the Lorentz force, the dynamic equation of motion turns into:

$$\frac{\partial \sigma_{rr}}{\partial r} + \frac{1}{r}(\sigma_{rr} - \sigma_{\theta\theta}) + F_r = \rho \left(\frac{\partial^2 u}{\partial t^2} - \Omega^2 u \right) \tag{17}$$

Assume that a very high and constant magnetic field $\boldsymbol{H}_0 = (0,\ 0, H_0)$ is immersed in the cylinder, and we also assume that $\boldsymbol{E} = 0$. Under these assumptions, from the generalized Ohm's law (8), we have:

$$J_z = 0. \tag{18}$$

Thus, the current density components J_r and J_θ are given as:

$$J_r = \frac{\sigma_0 \mu_0 H_0}{1+m^2}\left(m\frac{\partial u}{\partial t}\right),\ J_\theta = \frac{\sigma_0 \mu_0 H_0}{1+\ m^2}\left(-\frac{\partial u}{\partial t}\right). \tag{19}$$

The radial component of the Lorentz force F_r induced by the magnetic field $\boldsymbol{H}_0$ is given by:

$$F_r = \mu_0(\boldsymbol{J} \times \boldsymbol{H})_r. \tag{20}$$

Using Equations (14)–(16) and (18)–(20) in Equations (8), (9) and (17), the governing equations for the considered semiconducting medium are:

$$(\lambda+2\mu)\frac{\partial}{\partial r}\left(\frac{1}{r}\frac{\partial(ru)}{\partial r}\right) - \beta\frac{\partial T}{\partial r} - \delta_n\frac{\partial N}{\partial r} - \frac{\sigma_0\mu_0^2 H_0^2}{1+\ m^2}\left(\frac{\partial u}{\partial t}\right) = \rho\left(\frac{\partial^2 u}{\partial t^2} - \Omega^2 u\right), \tag{21}$$

$$\frac{\partial N}{\partial t} = D_E\left(\nabla^2 N\right) - \frac{N}{\tau} + \kappa T, \tag{22}$$

$$K\frac{\partial}{\partial t}\nabla^2 T + K^*\nabla^2 T + \frac{E_g \dot{N}}{\tau} = \left(1+\tau_0\frac{\partial}{\partial t}\right)\left[\rho C_E\frac{\partial^2 T}{\partial t^2} + \beta T_0\frac{\partial^2 e}{\partial t^2}\right]. \tag{23}$$

For the 1D problem, the Laplacian operator ∇^2 in the cylindrical coordinate is written as:

$$\nabla^2 \equiv \frac{\partial^2}{\partial r^2} + \frac{1}{r}\frac{\partial}{\partial r}.$$

Pre-operating both sides of Equation (21) by $\left(\frac{1}{r} + \frac{\partial}{\partial r}\right)$, yields:

$$(\lambda+2\mu)\nabla^2 e - \beta\nabla^2 T - \delta_n\nabla^2 N - \frac{\sigma_0\mu_0^2 H_0^2}{1+\ m^2}\left(\frac{\partial e}{\partial t}\right) = \left(\frac{\partial^2 e}{\partial t^2} - \Omega^2 e\right). \tag{24}$$

To represent the above equations in dimensionless form, the dimensionless quantities are given by:

$$\begin{gathered}(r', u') = v_0\eta(r,u), \quad \left(T', N', \sigma'_{ij},\ \Omega\,\prime\right) = \tfrac{1}{\rho v_0^2}\ (\beta T, \delta_n N, \sigma_{ij},\ \Omega), \quad (\tau_0', \tau', t') = v_0^2\eta(\tau_0, \tau, t), \\ \eta = \tfrac{\rho C_E}{K},\ \rho v_0^2 = \lambda+2\mu,\ M = \tfrac{\sigma_0\mu_0^2 H_0^2}{\eta\rho v_0^2},\ \gamma = \sqrt{\tfrac{\mu}{\lambda+2\mu}}.\end{gathered} \tag{25}$$

Here, the magnetic parameter M (also known as the Hartmann number) measures the strength of the magnetic field. Using (25) in Equations (21)–(23), after suppressing the primes, yields:

$$\nabla^2 e - \nabla^2 T - \nabla^2 N - \frac{M}{1+\ m^2}\left(\frac{\partial e}{\partial t}\right) = \left(\frac{\partial^2 e}{\partial t^2} - \Omega^2 e\right), \tag{26}$$

$$\frac{\partial N}{\partial t} = \delta_1\left(\nabla^2 N\right) - \delta_2 N + \delta_3 T, \tag{27}$$

$$\frac{\partial}{\partial t}\nabla^2 T + \delta_4\nabla^2 T + \delta_5\frac{\partial N}{\partial t} = \left(1+\tau_0\frac{\partial}{\partial t}\right)\left[\frac{\partial^2 T}{\partial t^2} + \delta_6\frac{\partial^2 e}{\partial t^2}\right], \tag{28}$$

where

$$\delta_1 = D_E\eta, \quad \delta_2 = \frac{1}{\tau}, \quad \delta_3 = \frac{\kappa\delta_n}{\beta}, \ \delta_4 = \frac{K^*}{(\lambda+2\mu)C_E}, \delta_5 = \frac{E_g}{\delta_n K v_0^2 \eta^2 \tau}, \quad \delta_6 = \frac{\beta^2 T_0}{\rho v_0^2 \eta}.$$

Using the dimensionless quantities defined by (25) in Equations (11)–(13), after suppressing the primes, yields:

$$\sigma_{rr} = 2\gamma^2 \frac{\partial u}{\partial r} + \left(1 - 2\gamma^2\right)e - (T+N), \tag{29}$$

$$\sigma_{\theta\theta} = 2\gamma^2 \frac{u}{r} + \left(1 - 2\gamma^2\right)e - (T+N), \tag{30}$$

$$\sigma_{zz} = \left(1 - 2\gamma^2\right)e - (T+N). \tag{31}$$

The initial conditions of the problem are taken as:

$$u(r,0) = 0 = \frac{\partial u}{\partial t}(r,0) \tag{32}$$

$$T(r,0) = 0 = \frac{\partial T}{\partial t}(r,0) \tag{33}$$

$$N(r,0) = 0 = \frac{\partial N}{\partial t}(r,0). \tag{34}$$

The Laplace transform of a function f with respect to the time variable t, with s as a Laplace transform variable, is defined as:

$$\mathcal{L}(f(t)) = \overline{f}(s) = \int_0^\infty f(t)e^{-st}dt. \tag{35}$$

Using Laplace transforms on Equation (35) to Equations (26)–(28), we obtain:

$$\left(\nabla^2 + \left(\Omega^2 - s^2\right) - \frac{Ms}{1+\ m^2}\right)\overline{e} - \nabla^2\overline{T} - \nabla^2\overline{N} = 0, \tag{36}$$

$$\left(\delta_1\nabla^2 - (\delta_2 + s)\right)\overline{N} + \delta_3\overline{T} = 0, \tag{37}$$

$$(1+\tau_0 s)\delta_6 s^2\overline{e} + \left(-(s+\delta_4)\nabla^2 + (1+\tau_0 s)s^2\right)\overline{T} - \delta_5 s\overline{N} = 0. \tag{38}$$

Using Laplace transforms as given by Equation (32) on Equations (29)–(31), we obtain:

$$\overline{\sigma}_{rr} = 2\gamma^2 \frac{\partial \overline{u}}{\partial r} + \left(1 - 2\gamma^2\right)\overline{e} - \left(\overline{T} + \overline{N}\right), \tag{39}$$

$$\overline{\sigma}_{\theta\theta} = 2\gamma^2 \frac{\overline{u}}{r} + \left(1 - 2\gamma^2\right)\overline{e} - \left(\overline{T} + \overline{N}\right), \tag{40}$$

$$\overline{\sigma}_{zz} = \left(1 - 2\gamma^2\right)\overline{e} - \left(\overline{T} + \overline{N}\right). \tag{41}$$

For the solution of Equations (33)–(35), we must have:

$$\left(\nabla^6 - B\nabla^4 + C\nabla^2 - D\right)\left(\overline{e}, \overline{T}, \overline{N}\right) = 0, \tag{42}$$

where

$$A = -\delta_1\delta_{11}, \ \ B = -(A\delta_7 - \delta_1\delta_{10} - \delta_1\delta_9 + \delta_8\delta_{11})/A,$$
$$C = (-\delta_3\delta_5 s + \delta_3\delta_9 - \delta_1\delta_7\delta_{10} + \delta_8\delta_7\delta_{11} + \delta_8\delta_{10} + \delta_8\delta_9)/A,$$
$$D = (\delta_3\delta_7\delta_5 s - \delta_8\delta_7\delta_{10})/A,$$

$$\delta_7 = \left(\Omega^2 - s^2\right) - \tfrac{Ms}{1+\,m^2}, \delta_8 = \delta_2 + s, \delta_9 = (1+\tau_0 s)\delta_6 s^2,$$
$$\delta_{10} = (1+\tau_0 s)s^2, \delta_{11} = -(s+\delta_4).$$

Equation (42) is a bicubic equation and can be written as:

$$\left(\nabla^2 - \lambda_1^2\right)\left(\nabla^2 - \lambda_2^2\right)\left(\nabla^2 - \lambda_3^2\right)\left(\bar{e}, \overline{T}, \overline{N}\right) = 0, \tag{43}$$

where $\lambda_i^2, i = 1,2,3$, are the roots of the equation

$$\left(\lambda^6 - B\lambda^4 + C\lambda^2 - D\right) = 0, \tag{44}$$

given by

$$\lambda_1^2 = \frac{1}{3}(2S\sin\varphi + B)$$
$$\lambda_2^2 = \frac{1}{3}\left(-S\sin\varphi - \sqrt{3}S\cos\varphi + B\right)$$
$$\lambda_3^2 = \frac{1}{3}\left(-S\sin\varphi + \sqrt{3}S\cos\varphi + B\right)$$

with

$$S = \sqrt{B^2 - 3C}, \varphi = \frac{1}{3}\sin^{-1}\left(-\frac{2B^3 - 9BC + 27D}{2S^3}\right).$$

The broad solution of Equation (43) can be written as:

$$\left(\bar{e}, \overline{T}, \overline{N}\right) = \sum_{i=1}^{3}(1, \zeta_i, \eta_i) g_i I_0(\lambda_i r), \tag{45}$$

where $I_n(\cdot)$ specifies the 2nd type of modified Bessel functions of order n.

Using Equation (45) in Equations (36)–(38) yields:

$$\zeta_i = \frac{-\left(\lambda_i^2 + \delta_7\right)\left(\delta_9\lambda_i^2 - \delta_5\right)}{\delta_3\delta_5 + \left(\delta_{11}\lambda_i^2 + \delta_{10}\right)\left(\delta_1\lambda_i^2 - \delta_8\right)}, \tag{46}$$

$$\eta_i = \frac{-\left(\lambda_i^2 + \delta_7\right)(\delta_3)}{\delta_3\delta_5 + \left(\delta_{11}\lambda_i^2 + \delta_{10}\right)\left(\delta_1\lambda_i^2 - \delta_8\right)}. \tag{47}$$

In the Laplace transform domain, displacement u can be denoted as:

$$\overline{u} = \sum_{i=1}^{3} \frac{1}{\lambda_i} g_i I_1(\lambda_i r). \tag{48}$$

We obtained Equation (48) with the help of the Bessel function relation:

$$\int x I_0(x) dx = x I_1(x). \tag{49}$$

Differentiating Equation (48) with r, we get:

$$\frac{\partial \overline{u}}{\partial r} = \sum_{i=1}^{3} g_i \left[I_0(\lambda_i r) - \frac{1}{\lambda_i r} I_1(\lambda_i r)\right]. \tag{50}$$

Thus, the final thermal stress solutions are generated in closed form as follows:

$$\overline{\sigma}_{rr} = \sum_{i=1}^{3} g_i \left\{ l_i I_0(\lambda_i r) - \frac{2\gamma^2}{\lambda_i r} I_1(\lambda_i r) \right\}, \tag{51}$$

$$\overline{\sigma}_{\theta\theta} = \sum_{i=1}^{3} g_i \left\{ \frac{2\gamma^2}{\lambda_i r} I_1(\lambda_i r) + l_i I_0(\lambda_i r) \right\}, \tag{52}$$

$$\overline{\sigma}_{zz} = \sum_{i=1}^{3} g_i l_i I_0(\lambda_i r), \tag{53}$$

$$l_i = \left(1 - 2\gamma^2 - (\zeta_i + \eta_i)\right)$$

4. Boundary Conditions

We presume that the cylinder's outside surface is compelled. Therefore, the mechanical boundary condition can be expressed as:

$$u(r,t) = 0, \quad \text{at } r = r_0. \tag{54}$$

Moreover, the boundary condition for variable heat flux (exponential laser pulsed heat) is applied to the boundary surface:

$$q_p = q_0 \frac{t^2}{16t_p^2} e^{-\frac{t}{t_p}}, \text{ at } r = r_0. \tag{55}$$

Using dimensionless variables (25) on Equation (3) yields:

$$\left(1 + \tau_0 \frac{\partial}{\partial t}\right) \dot{q}_p = -\left(\frac{\partial}{\partial t} + \delta_4\right) \frac{\partial T}{\partial r}. \tag{56}$$

Equations (55) and (56) give the following boundary condition:

$$\frac{q_0}{16t_p^2} \left(1 + \tau_0 \frac{\partial}{\partial t}\right) \frac{\partial}{\partial t} \left(t^2 e^{-\frac{t}{t_p}}\right) = -\left(\frac{\partial}{\partial t} + \delta_4\right) \frac{\partial T}{\partial r}, \tag{57}$$

at $r = r_0$.

"The carriers can reach the sample surface during the diffusion phase, with a finite probability of recombination". The boundary condition for the carrier density is:

$$D_E \frac{\partial N}{\partial r} = s_v N, \text{at } r = r_0. \tag{58}$$

Applying the Laplace transform on the boundary conditions (54), (57), and (58) yields:

$$\overline{u}(r_0, s) = 0, \tag{59}$$

$$\left.\frac{\partial \overline{T}}{\partial r}\right|_{r=r_0} = -\frac{q_0(1 + \tau_0 s)s}{8(1 + st_p)^3 (s + \delta_4)} = -\overline{G}(s), \tag{60}$$

$$D_E \left.\frac{\partial \overline{N}}{\partial r}\right|_{r=r_0} = s_v \overline{N}(r_0, s). \tag{61}$$

Using Equations (45) and (48) in Equations (59)–(61), we get:

$$\sum_{i=1}^{3} g_i \frac{1}{\lambda_i} I_1(\lambda_i r_0) = 0, \tag{62}$$

$$\sum_{i=1}^{3} g_i I_1(\lambda_i r_0) \zeta_i \lambda_i = -\frac{q_0(1 + \tau_0 s)st_p}{8(1 + st_p)^3 (s + \delta_4)} = -\overline{G}(s), \tag{63}$$

$$\sum_{i=1}^{3} \eta_i g_i \{D_E \lambda_i I_1(\lambda_i r_0) - s_v I_0(\lambda_i r_0)\} = 0. \tag{64}$$

The values of $g_i, i = 1,2,3$ can be obtained by solving Equations (62)–(64) by Cramer's rule:

$$g_i(s) = \frac{\Delta_i}{\Delta} \tag{65}$$

$$\Delta = \mathrm{G}_1[\mathrm{G}_5\mathrm{G}_9 - \mathrm{G}_8\mathrm{G}_6] - \mathrm{G}_2[\mathrm{G}_4\mathrm{G}_9 - \mathrm{G}_6\mathrm{G}_7] + \mathrm{G}_3[\mathrm{G}_4\mathrm{G}_8 - \mathrm{G}_5\mathrm{G}_7],$$
$$\Delta_1 = \overline{G}(s)[\mathrm{G}_2\mathrm{G}_9 - \mathrm{G}_8\mathrm{G}_3],$$
$$\Delta_2 = -\overline{G}(s)[\mathrm{G}_1\mathrm{G}_9 - \mathrm{G}_7\mathrm{G}_3],$$
$$\Delta_3 = \overline{G}(s)[\mathrm{G}_1\mathrm{G}_8 - \mathrm{G}_2\mathrm{G}_7],$$
$$\mathrm{G}_i = \frac{1}{\lambda_i}\phi_i,$$
$$\mathrm{G}_{i+3} = \phi_i\zeta_i\lambda_i,$$
$$\mathrm{G}_{i+6} = \eta_i\{D_E\lambda_i\phi_i - s_v\psi_i\},$$
$$I_1(\lambda_i r_0) = \phi_i,\ I_0(\lambda_i r_0) = \psi_i,\ i = 1,2,3.$$

Using the values of $g_i(s)$ from Equation (65) in Equations (45), (48) and (51)–(53), the various components of displacement, temperature distribution, carrier density, and stresses are:

$$\overline{u} = \frac{\overline{G}(s)}{\Delta}\left\{[\mathrm{G}_2\mathrm{G}_9 - \mathrm{G}_8\mathrm{G}_3]\frac{\theta_1}{\lambda_1} - [\mathrm{G}_1\mathrm{G}_9 - \mathrm{G}_7\mathrm{G}_3]\frac{\theta_2}{\lambda_2} + [\mathrm{G}_1\mathrm{G}_8 - \mathrm{G}_2\mathrm{G}_7]\frac{\theta_3}{\lambda_3}\right\}, \tag{66}$$

$$\overline{T} = \frac{\overline{G}(s)}{\Delta}\{[\mathrm{G}_2\mathrm{G}_9 - \mathrm{G}_8\mathrm{G}_3]\zeta_1\vartheta_1 - [\mathrm{G}_1\mathrm{G}_9 - \mathrm{G}_7\mathrm{G}_3]\zeta_2\vartheta_2 + [\mathrm{G}_1\mathrm{G}_8 - \mathrm{G}_2\mathrm{G}_7]\zeta_3\vartheta_3\}, \tag{67}$$

$$\overline{N} = \frac{\overline{G}(s)}{\Delta}\{[\mathrm{G}_2\mathrm{G}_9 - \mathrm{G}_8\mathrm{G}_3]\eta_1\vartheta_1 - [\mathrm{G}_1\mathrm{G}_9 - \mathrm{G}_7\mathrm{G}_3]\eta_2\vartheta_2 + [\mathrm{G}_1\mathrm{G}_8 - \mathrm{G}_2\mathrm{G}_7]\eta_3\vartheta_3\}, \tag{68}$$

$$\overline{\sigma_{rr}} = \frac{\overline{G}(s)}{\Delta}\{[\mathrm{G}_2\mathrm{G}_9 - \mathrm{G}_8\mathrm{G}_3](l_1\vartheta_1 - \mu_1) - [\mathrm{G}_1\mathrm{G}_9 - \mathrm{G}_7\mathrm{G}_3](l_2\vartheta_2 - \mu_2) + [\mathrm{G}_1\mathrm{G}_8 - \mathrm{G}_2\mathrm{G}_7](l_3\vartheta_3 - \mu_3)\}, \tag{69}$$

$$\overline{\sigma_{\theta\theta}} = \frac{\overline{G}(s)}{\Delta}\{[\mathrm{G}_2\mathrm{G}_9 - \mathrm{G}_8\mathrm{G}_3]\{\mu_1 + l_1\vartheta_1\} - [\mathrm{G}_1\mathrm{G}_9 - \mathrm{G}_7\mathrm{G}_3]\{\mu_2 + l_2\vartheta_2\} + [\mathrm{G}_1\mathrm{G}_8 - \mathrm{G}_2\mathrm{G}_7]\{\mu_3 + l_3\vartheta_3\}\}, \tag{70}$$

$$\overline{\sigma_{zz}} = \frac{\overline{G}(s)}{\Delta}\{[\mathrm{G}_2\mathrm{G}_9 - \mathrm{G}_8\mathrm{G}_3]l_1\vartheta_1 - [\mathrm{G}_1\mathrm{G}_9 - \mathrm{G}_7\mathrm{G}_3]l_2\vartheta_2 + [\mathrm{G}_1\mathrm{G}_8 - \mathrm{G}_2\mathrm{G}_7]l_3\vartheta_3\}, \tag{71}$$

where

$$\vartheta_i = I_0(\lambda_i r), \theta_i = I_1(\lambda_i r), \mu_i = \frac{2\gamma^2}{\lambda_i r}I_1(\lambda_i r),\ i = 1,2,3$$

5. Inversion of the Transforms

To obtain the result of the problem in the physical domain, transforms in Equations (66)–(71) are inverted using:

$$f(x,t) = \frac{1}{2\pi i}\int_{e^{-i\infty}}^{e^{+i\infty}} \widetilde{f}(x,s)e^{-st}ds. \tag{72}$$

Finally, we evaluate the integral in Equation (72) using Romberg's integration (Press et al. [34]) with adaptive step size.

6. Particular Cases

1. If $K^* \neq 0,\ K \neq 0$ and $\tau_0 \neq 0$ in Equations (66)–(71), the results for the MGTPT can be obtained with rotation and with the Hall effect.

2. If $K^* \neq 0$, $K \neq 0$ and $\tau_0 = 0$ in Equations (66)–(71), the results for the photo-thermal Green–Naghdi III theory (PGN-III) can be obtained with rotation and with the Hall effect.
3. If $K \neq 0$ and $\tau_0 = 0$ in Equations (66)–(71), the results for the photo-thermal Green–Naghdi II model (PGN-II) can be obtained with rotation and with the Hall effect.
4. If $\tau_0 = 0, K^* = 0$, in Equations (66)–(71), the results for the coupled photo-thermoelasticity theory (CPTE) are obtained with rotation and with the Hall effect.
5. If $K^* = 0$, in Equations (66)–(71), the results for the generalized Lord–Shulman photo-thermoelasticity model (PLS) is obtained with rotation and with the Hall effect.
6. If the magnetic field, i.e., $\mu_0 = H_0 = 0$ in Equations (66)–(71), we get results for the thermoelastic semiconducting solid with rotation.
7. If $\Omega = 0$ in Equations (66)–(71), we get results for the semiconducting magneto-thermoelastic solid with the Hall effect and without rotation.

7. Numerical Results and Discussion

To demonstrate the theoretical results and to show the effect of the Hall current, the rotation, and the effect of the modified photo-thermal heat equation (MGTPT) graphically using MATLAB software, isotropic silicon (Si) material is used, with its physical data [33] as follows:

$\lambda = 3.64 \times 10^{10}$ N m^{-2},
$\mu = 5.46 \times 10^{10}$ N m^{-2},
$\beta = 7.04 \times 10^{6}$ N m^{-2} deg^{-1},
$\delta_n = -9 \times 10^{-31}$ m^{-3},
$\rho = 2.33 \times 10^{3}$ Kg m^{-3},
$C_E = 695$ J Kg^{-1} K^{-1},
$K = 150$ W m^{-1} K^{-1},
$K^* = 1.54 \times 10^{2}$ Ws,
$D_E = 2.5 \times 10^{-3}$ m^2 s^{-1},
$\mu_0 = 4\pi \times 10^{-7}$ H m^{-1},
$T_0 = 300$ K,
$H_0 = 1$ J m^{-1} nb^{-1},
$\tau = 5 \times 10^{-5}$ s,
$N_0 = 10^{20}$ m^{-3},
$\epsilon 0 = 8.838 \times 10^{-12}$ F m^{-1},
$E_g = 1.11$ eV,
$\alpha_T = 3 \times 10^{-6}$ K^{-1},
$s_v = 2$ m s^{-1},
$H_0 = 10^{8}$ Col cm^{-1} s^{-1},
$\sigma_0 = 9.36 \times 10^{5}$ Col^2 C^{-1} m^{-1} s^{-1}.

Figure 2 depicts the variation in the radial displacement for MGTPT and PGN-III theories with the Hall effect and the rotation. It is noticed that in the presence of the Hall effect and the rotation with MGTPT theory, the radial displacement is minimal. However, in the absence of the Hall effect in MGTPT theory, the radial displacement is on the higher side as compared to MGTPT and PGN-III theories with and without the Hall effect and the rotation. Moreover, as radial distance increases, radial displacement increases. Figure 3 illustrates the variation in the temperature distribution for MGTPT and PGN-III theories with the Hall effect and the rotation. It is noticed that the temperature distribution is higher in the inner core of the cylinder as compared to the outer core of the cylinder. Moreover, the presence of the Hall effect causes a higher temperature distribution, and rotation results in a lower temperature distribution.

Figure 4 shows the variation in the carrier density for MGTPT and PGN-III theories with the Hall effect and the rotation. It is noticed that in the presence of the Hall effect and the rotation with MGTPT theory, the variation in the carrier density is minimal. However, PGN-III theory results in maximum variation in the carrier density. It is noticed that variation in the carrier density is higher in the inner core of the cylinder as compared to the outer core of the cylinder. Figures 5–7 show the variation in the stress components for MGTPT and PGN-III theories with the Hall effect and the rotation. It is noticed that in the presence of the Hall effect and the rotation with MGTPT theory, the variation in the stress components is minimum. However, PGN-III theory results in maximum variation in the stress components. It is noticed that variation in the stress components is higher in the inner core of the cylinder as compared to the outer core of the cylinder.

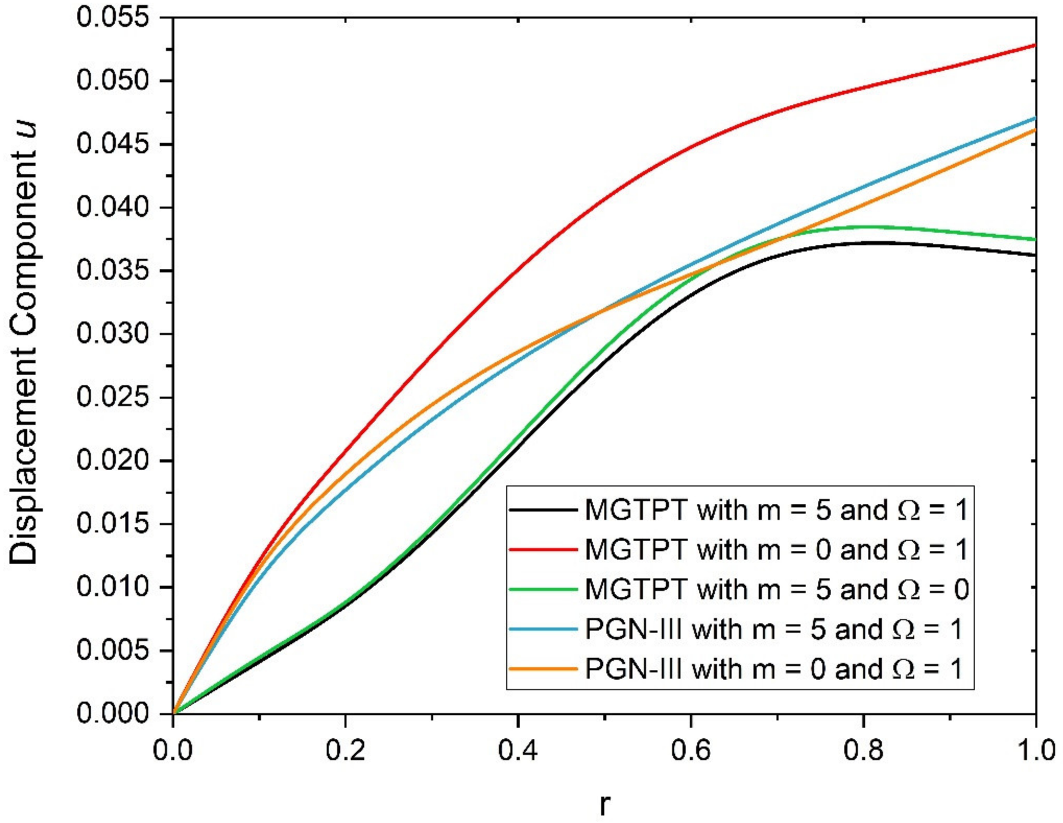

Figure 2. The radial displacement variation for various models with Hall effect and rotation.

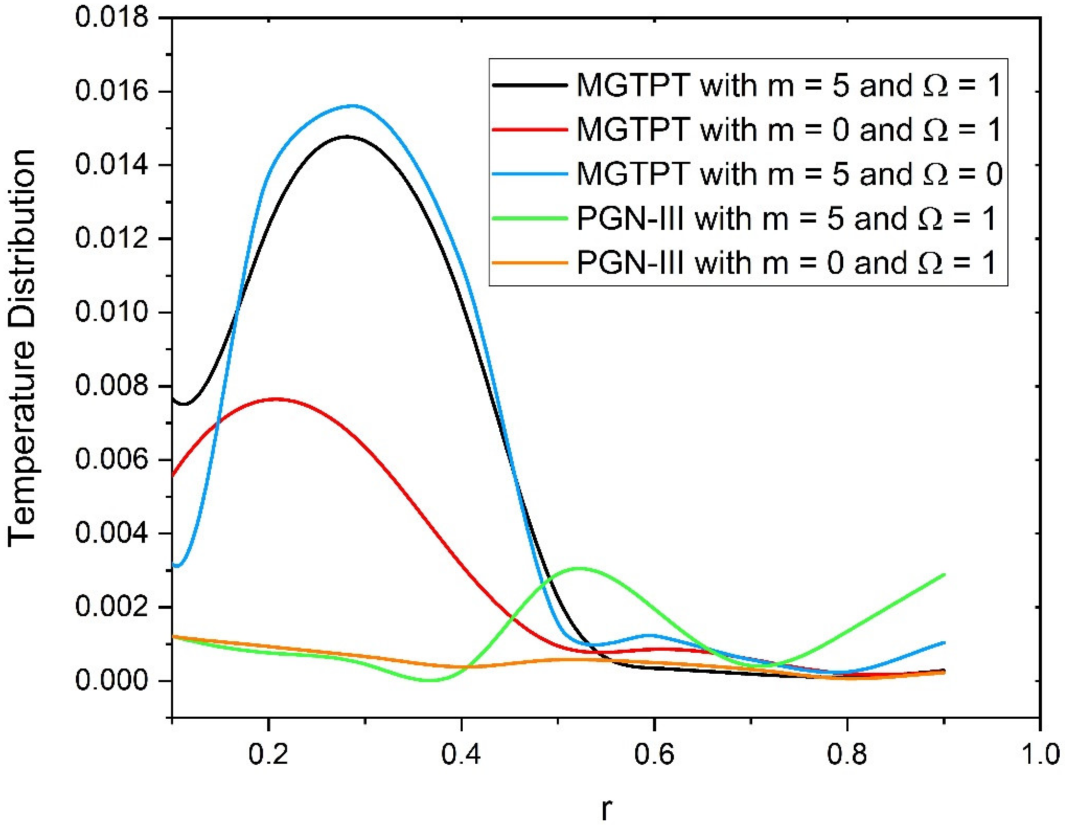

Figure 3. The temperature variation for various models with Hall effect and rotation.

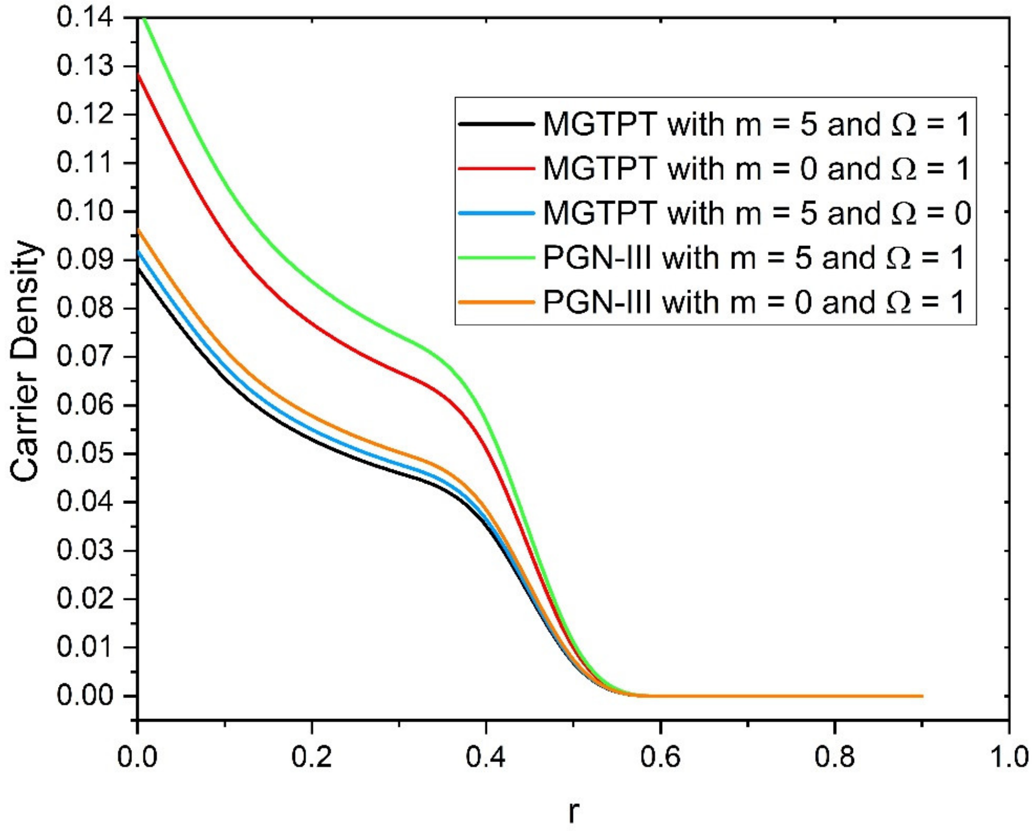

Figure 4. The variation in carrier density for various models with Hall effect and rotation.

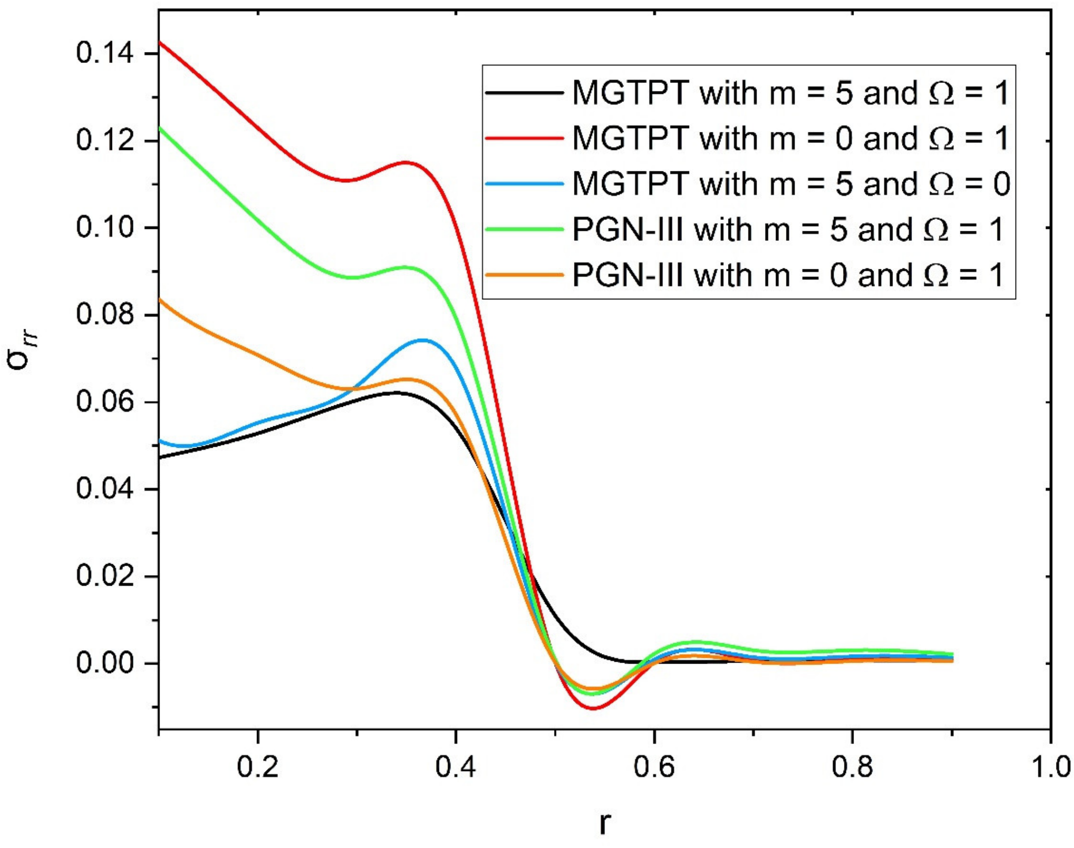

Figure 5. The deviation in radial stress for various models with Hall effect and rotation.

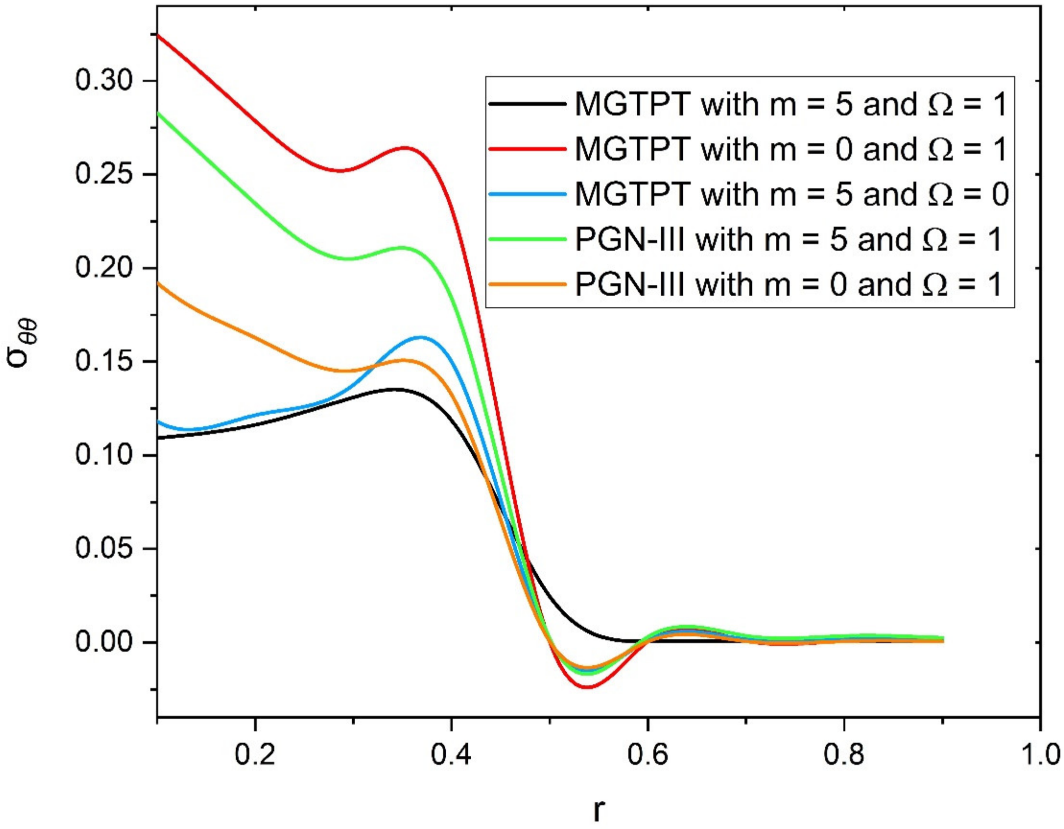

Figure 6. The deviation in hoop stress for various models with Hall effect and rotation.

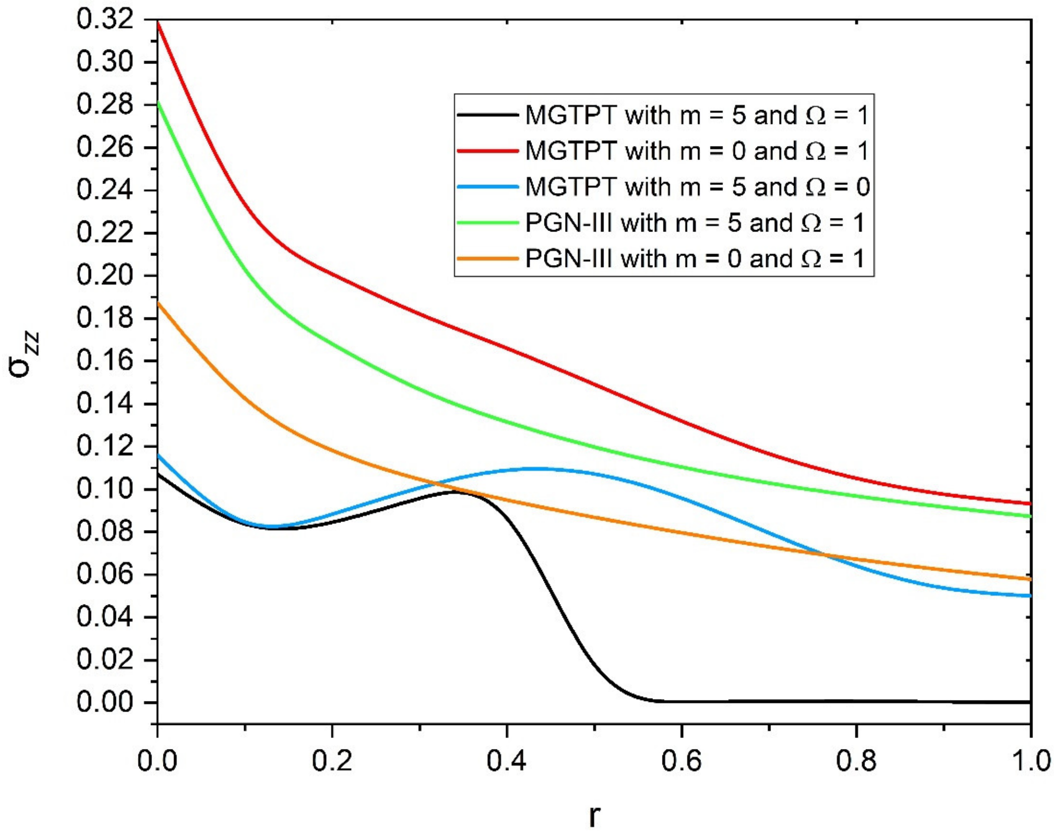

Figure 7. The deviation in vertical stress for various models with Hall effect and rotation.

8. Conclusions

This study lays out several photo-thermoelasticity models that are generalized in the Moore–Gibson–Thompson photo-thermal (MGTPT) model. In addition, the Green–Naghdi type III model is also included this study. Some of the physical consequences of some earlier models were solved by using this generalized model. In this study, we examined the rotating infinite semiconducting solid cylinder under a high magnetic field along its axis with an exponential laser pulse applied on its boundary surface. The semiconducting medium is rotating with angular frequency Ω and under a high magnetic field. The governing equations are expressed with the help of the Hall current, rotation, and MGTPT. As seen in the graphs, all the domains examined are significantly impacted by the Hall current and rotation. Photo-thermal methods are not only simple and sensitive, but can also be used to gain some insight into the process of de-excitation in materials and optical absorption. The ideas presented in this paper will be useful for physicists, material designers, thermal engineers, and geophysicists. A wide range of photo-thermoelasticity and thermodynamic problems can be solved using the technique used in the present study.

Author Contributions: I.K.: idea formulation, conceptualization, formulated strategies for mathematical modelling, methodology refinement, formal analysis, validation, and writing—review and editing. K.S.: Conceptualization, effective literature review, experiments and simulation, investigation, methodology, software, supervision, validation, visualization, and writing—original draft. E.-M.C.: conceptualization, effective literature review, formulated strategies for mathematical modelling, investigation, methodology, software, supervision, validation, visualization, and writing—review and editing. All authors have read and agreed to the published version of the manuscript.

Funding: This research received no external funding.

Data Availability Statement: For the numerical results, silicon material has been taken from Abouelregal and Atta [34].

Conflicts of Interest: The authors declare no conflict of interest.

Nomenclature

δ_{ij}	Kronecker delta	λ, μ	Lame's elastic constants
F_i	The body force	u_i	Components of displacement (m)
T	Thermodynamic temperature	D_E	Carrier diffusion coefficients
ρ	Medium density (Kg m^{-3})	e_{kk}	Cubical dilatation
N_0	Carrier concentration at equilibrium position	c_e	Electron charge
σ_{ij}	Stress tensors (N m^{-2})	E_g	Energy gap of the semiconductor parameter
e_{ij}	Strain tensors (mm^{-1})	J_i	Conduction current density tensor
N	Carrier density	Ω	Angular frequency
q_0	Constant	τ	Photo-generated carrier lifetime
t	Time	β_{ij}	Thermal elastic coupling tensor
t_e	Electron collision time	K_{ij}^*	Material constant
α_t	Linear thermal expansion coefficient	m	Hall effect parameter
δ_n	Electronic deformation coefficient	τ_0	Thermal relaxation parameter
K_{ij}	Coefficient of thermal conductivity	κ	Coupling parameter for thermal activation
d_n	Coefficient of electronic deformation	t_p	Pulsing heat flux duration time
ϵ_{ijk}	Permutation symbol	ω_e	Electron frequency
H_i	Intensity tensor of the magnetic field	T_0	Reference temperature s.t. $\lvert T/T_0 \rvert < < 1$
s_v	Surface recombination velocity	σ_0	Electrical conductivity
n_e	Electron number density	C_E	Specific heat at constant strain
m_e	Electron mass	E_i	Intensity tensor of the electric field
μ_0	Magnetic permeability		

References

1. Duhamel, J.M. Memories of the molecular actions developed by changes in temperatures in solids. *Mummy Div. Sav. Acad. Sci. Par.* **1938**, *5*, 440–498.
2. Biot, M.A. Thermoelasticity and Irreversible Thermodynamics. *J. Appl. Phys.* **1956**, *27*, 240–253. [CrossRef]
3. Cattaneo, C. A form of heat-conduction equations which eliminates the paradox of instantaneous propagation. *Comptes Rendus Acad. Sci. Paris Ser. II* **1958**, *247*, 431–433.
4. Vernotte, P. Les paradoxes de la theorie continue de l'equation de lachaleur. *Comptes Rendus Acad. Sci. Paris Ser. II* **1958**, *246*, 3154–3155.
5. Vernotte, P. Some possible complications in the phenomena of thermal conduction. *Comptes Rendus Acad. Sci. Paris Ser. II* **1961**, *252*, 2190–2191.
6. Lord, H.W.; Shulman, Y. A generalized dynamical theory of thermoelasticity. *J. Mech. Phys. Solids* **1967**, *15*, 299–309. [CrossRef]
7. Green, A.E.; Lindsay, K.A. Thermoelasticity. *J. Elast.* **1972**, *2*, 1–7. [CrossRef]
8. Dhaliwal, R.S.; Sheriff, H.H. Generalized Thermoelasticity for Anisotropic Media. *Q. Appl. Math.* **1980**, *38*, 1–8. [CrossRef]
9. Green, A.E.; Naghdi, P.M. A re-examination of the basic postulates of thermomechanics. *Proc. R. Soc. London. Ser. A Math. Phys. Sci.* **1991**, *432*, 171–194. [CrossRef]
10. Green, A.E.; Naghdi, P.M. On undamped heat waves in an elastic solid. *J. Therm. Stresses* **1992**, *15*, 253–264. [CrossRef]
11. Green, A.E.; Naghdi, P.M. Thermoelasticity without energy dissipation. *J. Elast.* **1993**, *31*, 189–208. [CrossRef]
12. Lasiecka, I.; Wang, X. Moore–Gibson–Thompson equation with memory, part II: General decay of energy. *J. Differ. Equ.* **2015**, *259*, 7610–7635. [CrossRef]
13. Quintanilla, R. Moore–Gibson–Thompson thermoelasticity. *Math. Mech. Solids* **2019**, *24*, 4020–4031. [CrossRef]
14. Quintanilla, R. Moore-Gibson-Thompson thermoelasticity with two temperatures. *Appl. Eng. Sci.* **2020**, *1*, 100006. [CrossRef]
15. Fernández, J.R.; Quintanilla, R. Moore-Gibson-Thompson theory for thermoelastic dielectrics. *Appl. Math. Mech.* **2021**, *42*, 309–316. [CrossRef]
16. Bazarra, N.; Fernández, J.; Quintanilla, R. Analysis of a Moore–Gibson–Thompson thermoelastic problem. *J. Comput. Appl. Math.* **2020**, *382*, 113058. [CrossRef]
17. Marin, M. On weak solutions in elasticity of dipolar bodies with voids. *J. Comput. Appl. Math.* **1997**, *82*, 291–297. [CrossRef]
18. Lata, P.; Kaur, I. Thermomechanical interactions in transversely isotropic magneto-thermoelastic medium with fractional order generalized heat transfer and Hall current. *Arab J. Basic Appl. Sci.* **2019**, *27*, 13–26. [CrossRef]
19. Lotfy, K.; El-Bary, A.A. Thomson effect in thermo-electro-magneto semiconductor medium during photothermal excitation process. *Waves Random Complex Media* **2020**, *32*, 1–19. [CrossRef]
20. Mahdy, A.; Lotfy, K.; Ahmed, M.; El-Bary, A.; Ismail, E. Electromagnetic Hall current effect and fractional heat order for microtemperature photo-excited semiconductor medium with laser pulses. *Results Phys.* **2020**, *17*, 103161. [CrossRef]
21. Kaur, I.; Singh, K. Fractional order strain analysis in thick circular plate subjected to hyperbolic two temperature. *Partial. Differ. Equ. Appl. Math.* **2021**, *4*, 100130. [CrossRef]
22. Kaur, I.; Singh, K. Plane wave in non-local semiconducting rotating media with Hall effect and three-phase lag fractional order heat transfer. *Int. J. Mech. Mater. Eng.* **2021**, *16*, 16. [CrossRef]
23. Marin, M.; Craciun, E.M.; Pop, N. Some Results in Green–Lindsay Thermoelasticity of Bodies with Dipolar Structure. *Mathematics* **2020**, *8*, 497. [CrossRef]
24. Marin, M.; Othman, M.I.A.; Abbas, I.A. An Extension of the Domain of Influence Theorem for Generalized Thermoelasticity of Anisotropic Material with Voids. *J. Comput. Theor. Nanosci.* **2015**, *12*, 1594–1598. [CrossRef]
25. Kaur, I.; Lata, P.; Singh, K. Effect of Hall current in transversely isotropic magneto-thermoelastic rotating medium with fractional-order generalized heat transfer due to ramp-type heat. *Indian J. Phys.* **2020**, *95*, 1165–1174. [CrossRef]
26. Bhatti, M.M.; Ellahi, R.; Zeeshan, A.; Marin, M.; Ijaz, N. Numerical study of heat transfer and Hall current impact on peristaltic propulsion of particle-fluid suspension with compliant wall properties. *Mod. Phys. Lett. B* **2019**, *33*, 1950439. [CrossRef]
27. Bhatti, M.M.; A Yousif, M.; Mishra, S.R.; Shahid, A. Simultaneous influence of thermo-diffusion and diffusion-thermo on non-Newtonian hyperbolic tangent magnetised nanofluid with Hall current through a nonlinear stretching surface. *Pramana* **2019**, *93*, 88. [CrossRef]
28. Othman, M.I.; Marin, M. Effect of thermal loading due to laser pulse on thermoelastic porous medium under G-N theory. *Results Phys.* **2017**, *7*, 3863–3872. [CrossRef]
29. Marin, M.; Othman, M.I.A.; Seadawy, A.R.; Carstea, C. A domain of influence in the Moore–Gibson–Thompson theory of dipolar bodies. *J. Taibah Univ. Sci.* **2020**, *14*, 653–660. [CrossRef]
30. Craciun, E.-M.; Baesu, E.; Soós, E. General solution in terms of complex potentials for incremental antiplane states in prestressed and prepolarized piezoelectric crystals: Application to Mode III fracture propagation. *IMA J. Appl. Math.* **2004**, *70*, 39–52. [CrossRef]
31. Lotfy, K.; El-Bary, A.; Hassan, W.; Ahmed, M. Hall current influence of microtemperature magneto-elastic semiconductor material. *Superlattices Microstruct.* **2020**, *139*, 106428. [CrossRef]
32. Abouelregal, A.E.; Mohammad-Sedighi, H.; Shirazi, A.H.; Malikan, M.; Eremeyev, V.A. Computational analysis of an infinite magneto-thermoelastic solid periodically dispersed with varying heat flow based on non-local Moore–Gibson–Thompson approach. *Contin. Mech. Thermodyn.* **2021**, *34*, 1067–1085. [CrossRef]

33. Abouelregal, A.E.; Atta, D. A rigid cylinder of a thermoelastic magnetic semiconductor material based on the generalized Moore–Gibson–Thompson heat equation model. *Appl. Phys. A* **2022**, *128*, 118. [CrossRef]
34. Press, W.H.; Teukolsky, S.A.; Flannery, B.P. *Numerical Recipes in Fortran*; Cambridge University Press: Cambridge, UK, 1980.